The new low-toxic histone deacetylase inhibitor S-(2) induces apoptosis in various acute myeloid leukemia cells

(Article begins on next page)

The new low-toxic histone deacetylase inhibitor *S*-(2) induces apoptosis in various acute myeloid leukaemia cells

C. Cellai [a], M. Balliu [a], A. Laurenzana [a], L. Guandalini [b], R. Matucci [c], D. Miniati [c], E. Torre [a], A. Nebbioso [d], V. Carafa [d], L. Altucci [d], M. N. Romanelli [b], F. Paoletti [a], *

[a] *Department of Experimental Pathology and Oncology, University of Florence, Italy*
[b] *Department of Pharmaceutical Sciences, University of Florence, Sesto Fiorentino, Italy*
[c] *Department of Preclinical and Clinical Pharmacology, University of Florence, Italy*
[d] *Department of General Pathology, Seconda Università degli Studi di Napoli, Italy*

Abstract

Histone deacetylase inhibitors (HDACi) induce tumor cell cycle arrest and/or apoptosis, and some of them are currently used in cancer therapy. Recently, we described a series of powerful HDACi characterized by a 1,4-benzodiazepine (BDZ) ring hybridized with a linear alkyl chain bearing a hydroxamate function as Zn^{++}-chelating group. Here, we explored the anti-leukaemic properties of three novel hybrids, namely the chiral compounds *(S)*-**2** and *(R)*-**2**, and their non-chiral analogue **4**, which were first comparatively tested in promyelocytic NB4 cells. *(S)*-**2** and partially **4** – but not *(R)*-**2** – caused G0/G1 cell-cycle arrest by up-regulating cyclin G2 and p21 expression and down-regulating cyclin D2 expression, and also apoptosis as assessed by cell morphology and cytofluorimetric assay, histone H2AX phosphorylation and PARP cleavage. Notably, these events were partly prevented by an anti-oxidant. Moreover, novel HDACi prompted p53 and α-tubulin acetylation and, consistently, inhibited HDAC1 and 6 activity. The rank order of potency was *(S)*-**2** > **4** > *(R)*-**2**, reflecting that of other biological assays and addressing *(S)*-**2** as the most effective compound capable of triggering apoptosis in various acute myeloid leukaemia (AML) cell lines and blasts from patients with different AML subtypes. Importantly, *(S)*-**2** was safe in mice (up to 150 mg/kg/week) as determined by liver, spleen, kidney and bone marrow histopathology; and displayed negligible affinity for peripheral/central BDZ-receptors. Overall, the BDZ-hydroxamate *(S)*-**2** showed to be a low-toxic HDACi with powerful anti-proliferative and pro-apototic activities towards different cultured and primary AML cells, and therefore of clinical interest to support conventional anti-leukaemic therapy.

Keywords: HDAC inhibitors (HDACi) • benzodiazepine (BDZ) • acute myeloid leukaemia (AML) • cell growth arrest • apoptosis • H2AX • PARP • *in vivo* toxicity

Introduction

The balance between histone acetyl-transferase (HATs) and histone deacetylase (HDACs) activities is known to play a significant role in chromatin remodeling and epigenetic regulation of gene expression in several diseases. In cancer, HATs are often functionally inactivated or mutated while over-expression of many HDACs has been reported [1–4]. Therefore, HDACs have become attractive chemotherapy targets for a range of structurally diverse natural or synthetic agents – hydroxamates, cyclic peptides, electrophilic ketones, short-chain fatty acids and benzamides [5, 6] – acting as HDAC inhibitors (HDACi). These epigenetic agents are known to induce: (*i*) acetylation of histones – that is functional to a chromatin relaxed status and proper interaction of transcription factors to DNA elements – as well as of nonhistone proteins [7]; and (*ii*) cell growth arrest and/or apoptosis in several cancer models through the activation of multiple pathways including generation of reactive oxygen species (ROS), inhibition of angiogenesis and increase in autophagy [5]. However, regardless of specific action mechanisms of HDACi, their greater activity in cancer cells relative to normal cells has widely been recognized [4, 8] and some of them are currently employed in the clinic as monotherapy and/or in combination with conventional anti-neoplastic agents

*Correspondence to: Prof. Francesco PAOLETTI, Ph.D.,
Department of Experimental Pathology and Oncology,
Viale G.B. Morgagni 50, 50134 – Firenze, Italy.
Tel.: +39-055-4598-212
Fax: +39-055-4598-903
E-mail: francesco.paoletti@unifi.it

[5, 9]. Vorinostat is the first HDACi approved by the FDA for treatment of cutaneous T-cell lymphoma [5, 10], but also MS-275, romidepsin and valproic acid are now in phases I/III of clinical trials to treat different types of human cancers.

Recently, we reported and preliminarily assayed in acute promyelocytic leukaemia NB4 cells a wide series of powerful HDACi characterized by a 1,4-benzodiazepine ring (BDZ) used as the cap and joined, through an amide function or a triple bond connection unit, to a linear alkyl chain carrying a hydroxamate moiety as the Zn^{++}-chelating group [11]. The present study focuses on three novel HDACis, namely the chiral compounds *(S)*-**2** and *(R)*-**2,** and their non-chiral analogue **4**, which have comparatively been tested for their ability to induce growth arrest and apoptosis in NB4 cells, and to target specific HDAC isoforms. Taken together, our results point to *(S)*-**2** as the most effective among the three hybrids to trigger apoptosis in various acute myeloid leukaemia (AML) cell lines and blasts from patients with different AML subtypes [12]. Furthermore, *(S)*-**2** was safe for normal CD-1 mice up to 150 mg/kg/week along with acute toxicity experiments as revealed by histopathology of explanted organs and showed no affinity for central (CBR) and peripheral BDZ receptors (PBR). These findings confirm the anti-leukaemic efficacy and safety of *(S)*-**2**, which may offer interesting clinical opportunities to treat AML and, possibly, other types of malignancies.

Materials and methods

Cell lines, blasts and culture conditions

Different AML cell lines, including KG1a, Kasumi, HL-60, ATRA-sensitive NB4 and ATRA-resistant NB4-MR4, THP-1 and U937 were employed and cultured as previously reported [13]. Blasts from bone marrow aspirate and/or peripheral blood of newly diagnosed AML patients with M1-M4 subtypes as well as peripheral mononuclear blood cells (PMBCs) from normal subjects were obtained after informed consent and according to the Hospital Committee Ethics guidelines (Helsinki declaration). Blasts and PBMCs were isolated and cultured as described elsewhere [14].

Reagents

The 1,4-benzodiazepine ring (5-phenyl-1,3-dihydro-2-oxo-benzo[e][1,4]-diazepine) was used as the cap of novel hydroxamic-based HDACi [11]. The chiral compounds (*S*)-**2** and (*R*)-**2**, and their non-chiral analogue **4** (Fig. 1) were dissolved in dimethyl sulfoxide (DMSO; Sigma-Aldrich, St Louis, MO, USA), stored as 0.1 M stock solutions in the dark at room temperature and added directly to the culture. The amount of DMSO used as the vehicle did not interfere with drug biological activities. All other chemicals were reagent grade.

RNA extraction, RT-PCR and QRT-PCR experiments

For details on methodologies and the primers used see Supporting Information (S1)
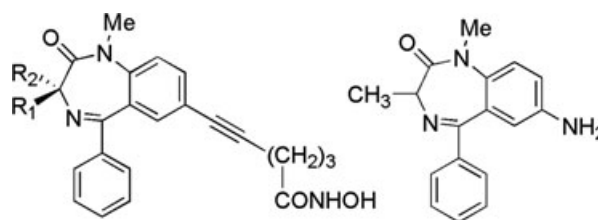
Fig. 1 Chemical structures of compounds used in this work. The numbers labelling the compounds are the same as in ref. [11].

Cell extraction, SDS-PAGE and Western blotting

Harvested cells were resuspended in a lysis buffer (1 mM phenylmethyl-sulfonyl fluoride, 1% Triton X-100, 40 mM Tris–HCl pH 8.0, 150 mM NaCl) containing a cocktail of proteinase inhibitors (Calbiochem, Merck KGaA, Darmstadt, Germany) and treated by sonication (Microson XL-2000, Misonix, Farmingdale, NY, USA). Proteins were assayed by the BCA Protein Assay (Thermo Scientific, Rockford, IL, USA), analysed by SDS-PAGE and Western blotting as reported elsewhere [13]. Membranes were probed with primary antibodies against p53 (Abcam, Cambridge, UK); acetyl-H3, acetyl-H4, acetyl-p53 and H4 (Upstate Biotechnology, Millipore, Bilerica, MA, USA); PARP, γ-H2AX, H2AX, H3 (Cell Signaling Technology, Danvers, MA. USA); α-tubulin and acetylated α-tubulin (Sigma-Aldrich, ST. Louis, MO, USA). Suitable peroxidase-conjugated IgG preparations (Sigma-Aldrich) were used as secondary antibodies; the ECL procedure was employed for development.

Cell cycle analysis and determination of apoptosis

Cell cycle distribution was measured by using the propidium iodide (PI)-hypotonic citrate method with a FACScan flow cytometer (Becton-Dickinson, San Jose, CA, USA) [15]. Apoptosis was assessed either cytofluorimetrically by using the Annexin-V-Fluos/PI assay (Roche Molecular Biochemicals, Mannheim, Germany), or morphologically by examining May-Grünwald/Giemsa stained cytosmears as reported elsewhere [13].

Determination of HDAC enzyme activity

The sensitivity of human recombinant HDAC1 and 6 enzymes to novel HDACi was assessed by fluorimetric assays (Supporting Information, S2) using the Boc-L-Lys(-acetyl)-MCA and the Boc-L-Lys(-trifluoroacetyl)-MCA as the substrates [16].

Acute toxicity experiments

Different groups of CD-1 mice were collected and treated with either DMSO as the vehicle or increasing amounts of (*S*)-**2** and **4** given i.p. up to

Fig. 2 Biological effects of (*S*)-**2**, (*R*)-**2** and **4** on NB4 cells. (**A**) Growth curves: NB4 cells (1×10^{-5}/ml) were incubated up to 96 hrs without/with increasing concentrations of either (*S*)-**2**, (*R*)-**2** or **4**. Cells densities were evaluated daily with the aid of a Bürker chamber and reported as results of a typical experiment out of three. (**B**) Cell cycle analysis was performed on propidium iodide (PI)-stained NB4 cells treated without/with 2 μM drugs for 24 hrs, by flow cytometry (PI labelling, X-axis; total events, Y-axis). (**C**) Cyclin D2, cyclin G2 and p21 mRNA levels from cells treated without/with 2 μM drugs for 6, 15 and 24 hrs were measured by quantitative reverse transcriptase polymerase chain reaction (RT-PCR; see Supporting Information, S1). Columns and bars were the means $\pm$ SD of three separate experiments and asterisks indicated the significant differences between treated and untreated cells (*** $P < 0.001$; * $P < 0.05$).
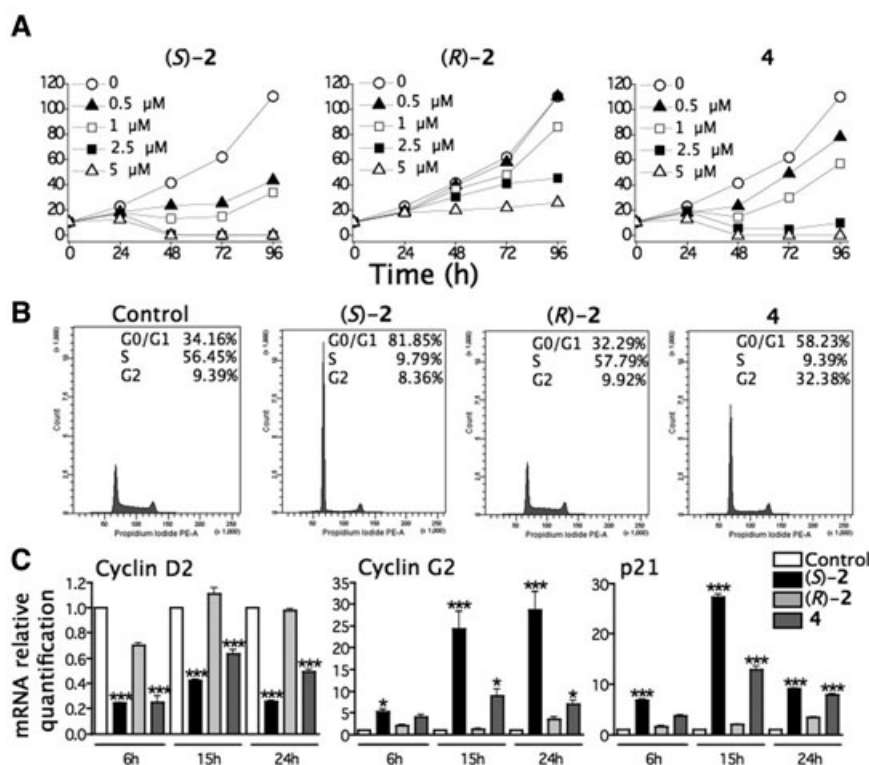
150 mg/Kg (about 5 mg/mouse). Animals were sacrificed after 7 days for histopathological evaluation of liver, kidney, spleen and bone marrow (Supporting Information, S3).

Binding experiments

The relative affinities of *rac*-**7** (as an example of the cap in its racemic form), (*S*)-**2**, (*R*)-**2**, and **4** for CBR and PBR, respectively were assessed [17, 18] and evaluated quantitatively with the weighted least-squares iterative curve fitting program LIGAND [19] (Supporting Information, S4).

Statistical analysis

Other data were analysed by Student's *t*-test. Significance was determined by analysis of variance followed by Newman-Keuls post-tests using Prism version 4.0 (GraphPad software, San Diego, CA, USA).

Results

Compounds used in this study

The rationale for generating novel BDZ-hydroxamate hybrids with HDACi activity has been previously described [11] and the molec-

ular structures of compounds used in this work were reported (Fig. 1). Briefly, the 1,4-benzodiazepine ring containing a chiral centre in position 3 was used as the cap and joined through a triple bond connection unit to a linear alkyl chain ending with a hydroxamic function, partially mimicking oxamflatin [20]. In this way, the BDZ-hydroxamate enantiomers (*S*)-**2** and (*R*)-**2** as well as their non-chiral analogue lacking the 3-methyl group on the cap and indicated as compound **4** were obtained.

Effects of novel HDACi on NB4 cell growth and cell cycle distribution

BDZ-hybrids have already been reported to induce acetylation of histone H3 and H4 in NB4 cells [11]. In the present work all three novel HDACi were found to be able, though with different potency, to inhibit cell growth in a dose- and time-dependent manner (Fig. 2A). (*S*)-**2** and **4** were the more effective agents ($IC_{50} = 0.41$ and 0.98 μM, respectively) after 72 hrs of treatment, while (*R*)-**2** was much less active ($IC_{50} = 3.81$ μM).

Cell cycle analysis at 24 hrs (Fig. 2B) showed that (*S*)-**2** caused a striking arrest of cells in G0/G1 (approximately 82% *versus* 34% of control) and a marked decrease in S phase, while cell cycle profiles of (*R*)-**2**-treated and control cells virtually overlapped. Compound **4** was less potent than (*S*)-**2** in arresting cell growth but, interestingly, led to a partial cell blockage in G2. These
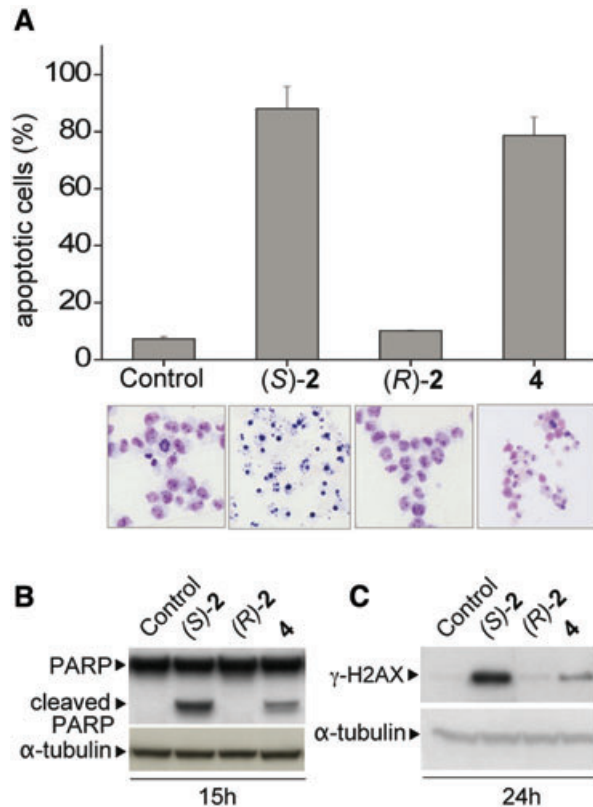
Fig. 3 (**A**-top) Cytofluorimetric analysis of apoptosis. NB4 cells were treated without/with 2.5 μM drugs for 48 hrs and incubated with AnnexinV-Fluos in a HEPES buffer containing PI for 15 min.; the number of apoptotic cells was then measured by flow cytometry (FACScan equipment). X axis: % of apoptotic cells; Y axis: conditions of stimulation; bars were the means $\pm$ SD of three separate experiments. (**A**-bottom) Cell morphology. Cytosmears of untreated and drug-treated NB4 cells as above were stained with May-Grünwald/Giemsa. Pictures (magnification: $\times$200) were from a typical experiment out of three. Drug-induced PARP cleavage (at 15 hrs, panel **B**) to yield a fragment of approximately 89 kD, and H2AX phosphorylation (at 24 hrs, panel **C**) were observed by Western blot and immunostaining; α-tubulin was used as the reference protein.

findings are consistent with molecular biology data showing that at all the time points within 24 hrs (*S*)-**2** and **4** were able to up-regulate cyclin G2 and p21 expression, and down-regulate cyclin D2 expression, whereas (*R*)-**2** was nearly ineffective (Fig. 2C).

BDZ-hybrids *(S)*-2 and 4, but not *(R)*-2, induce apoptosis in NB4 cells

Pro-apoptotic efficacy of (*S*)-**2** and **4**, as measured by flow cytometry after a 2-day treatment with 2.5 μM, was high and accounted for approximately 90% and 80% of cell population, respectively, while (*R*)-**2** did not alter cell viability relative to control (Fig. 3A,

top). Examination of stained cytosmears confirmed the massive nuclear fragmentation in (*S*)-**2**-treated cultures that depicts a late apoptotic stage, while cell shrinking, to suggest an early apoptotic phase, was the predominant feature in **4**-treated cultures (Fig. 3A, bottom). Moreover, pro-apoptotic properties of (*S*)-**2** and **4** were also proven by the cleavage of poly(ADP-ribose)-polymerase (PARP) as the ultimate target of the caspase cascade (Fig. 3B) and producing to generate a fragment of approximately 89 kD and, subsequently, by histone H2AX phosphorylation to yield γ-H2AX (Fig. 3C) in response to drug-mediated DNA damage [21]; these events did not occur in either untreated or (*R*)-**2**-treated cells.

## Drugs induce acetylation of histone and nonhistone proteins and inhibit HDAC1 and 6 enzymatic activity

Western blot analyses carried out on NB4 cells confirmed, as previously reported [11], that a 6-hr incubation with (*S*)-**2** and **4** caused histone H3/H4 acetylation, while (*R*)-**2** was definitely less active (Fig. 4A). However, nonhistone proteins like α-tubulin and p53 also underwent drug-induced acetylation, as detected after 6-hr and 24-hr treatment, respectively (Fig. 4B). Acetylated α-tubulin is a well-known substrate for the mainly cytoplasmic class IIb enzyme HDAC6 [22] and acetylated p53 is a specific substrate for the primarily nuclear class I enzyme HDAC1 [23], thus inferring that these two isoforms were sensitive targets for (*S*)-**2** and **4**. Consistently, novel hybrids were capable of inhibiting enzymatic activity of recombinant human HDAC1 and 6, as measured by a fluorimetric cell-free assay [16], to yield IC$_{50}$ values that were within a low micromolar range (Fig. 4C); the rank order of potency was (*S*)-**2** > **4** > (*R*)-**2** reflecting somewhat that observed in cell-based assays.

(S)-2 triggers apoptosis in different cultured and primary AML cells: preliminary evidence for ROS-mediated cell death

Since (*S*)-**2** exhibited the greatest HDACi activity and pro-apoptotic potency in NB4 cells, its efficacy was explored further in different AML cell lines. Cells were incubated with/out increasing (*S*)-**2** concentrations for 48 hrs and then submitted to the Annexinn V/PI assay to determine the amount of apoptotic cells within the population (Fig. 5A). Kasumi cells appeared to be especially sensitive to the drug (IC$_{50}$ = 0.61 μM), followed by KG1a, HL-60, NB4 and ATRA-resistant NB4-MR4 cells (IC$_{50}$ within a range of 1.4–2.1 μM) while U937 and THP-1 yielded values of 4.5 and 6.5 μM, respectively.

Pro-apoptotic effectiveness of (*S*)-**2** over such a wide range of different cultured AML cell lines prompted us to investigate on action mechanisms of drug-induced apoptosis. Toward this aim, NB4 cells were treated with/out 2 μM (*S*)-**2** for 15 hrs either in the absence or in the presence of 15 mM anti-oxidant N-Acetyl

Cysteine (NAC) applied 2 hrs before adding the drug. As expected, (S)-2 caused the cleavage of PARP resulting from activation of the caspase cascade, and the appearance of γ-H2AX due to drug-induced DNA damage. Both these events were inhibited by the presence of NAC to highlight the major role of ROS in drug-mediated cell death (Fig. 5B).
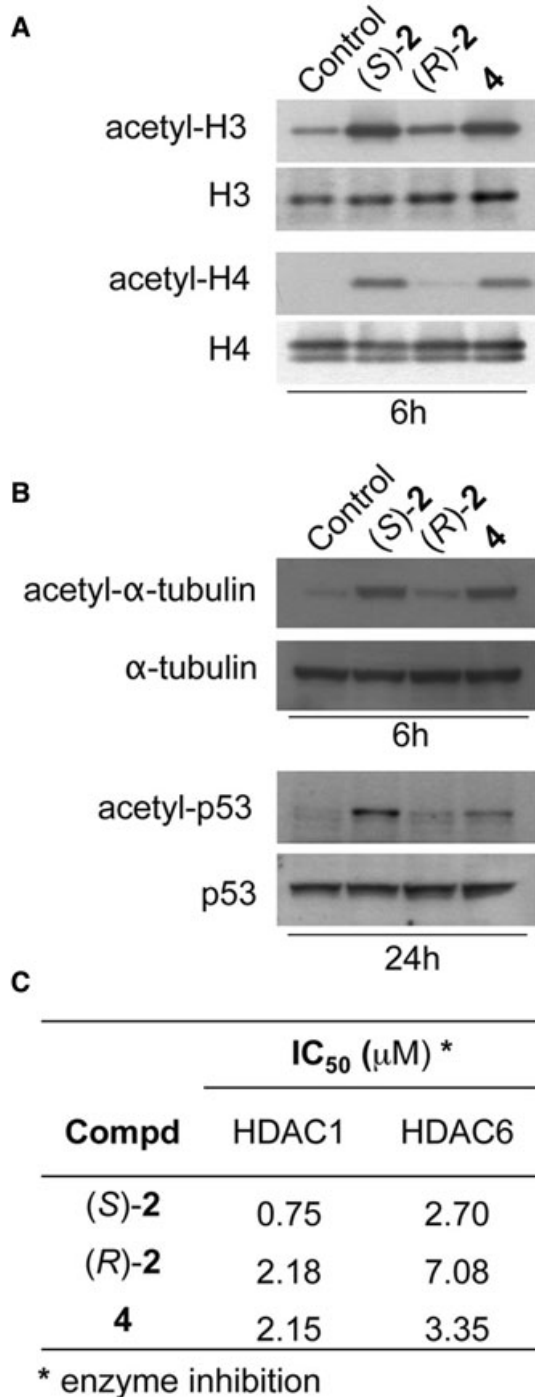
Pro-apoptotic properties of (S)-2 were also explored *ex vivo* in cultured blasts from patients with different AML (M1–M4) subtypes by using peripheral mononuclear blood cells (PBMCs) from normal subjects as the control. Cells treated for 48 hrs with/out 1 and 2 μM drug were collected, fixed and stained with May-Grünwald/Giemsa. There was a dose-dependent increase in apoptotic cells in cytosmears of all the treated AML samples; blasts of M1 and M2 subtype seemed to be especially drug-sensitive, while normal PMBCs were unaffected by the drug (Fig. 5C).

(S)-2 has a low-toxic profile *in vivo*

Normal CD-1 mice were used as the model for acute toxicity experiments. Animals were injected i.p. only once with increasing (S)-2 concentrations dissolved in 0.1 ml DMSO (see legend to Fig. 6A and Supporting Information, S3). All the mice displayed an increase in weight and excellent survival rates within a week despite the dosage. Moreover, the histopathology of bone marrow, liver, spleen and kidney specimens from mice receiving either the vehicle or the higher (S)-2 dosage (about 150 mg/Kg; *i.e.* 5 mg/mouse) revealed no specific drug-induced damage such as cell loss, necrotic areas or other signs of acute toxicity relative to controls (Fig. 6A). A slight vacuolization in liver and kidney parenchimal cells of both treated and untreated mice was observed and due, conceivably, to hypoxic conditions at sacrifice. Notably, similar results were obtained by replacing (S)-2 with comparable amounts of non-chiral compound **4** (data not shown).

(S)-2, (R)-2 and 4 show virtually no affinity for both CBR and PBR

Novel HDACi were tested in tissue extracts (Supporting Information, S4) for their ability to bind CBR or PBR by using Ro 15–1788 and PK 11195 as the specific ligand, respectively, and diazepam as the common ligand (Fig. 6B). At the two concentrations used (S)-2, (R)-2 and **4** showed virtually no affinity for both CBR and PBR as compared to the high affinity of Ro 15–1788 and diazepam for CBR and of PK 11195 and diazepam for PBR. The racemic BDZ cap (*rac*-**7**) due to its structural similarity to diazepam and the lack of the hydroxamic moiety showed a partial ability to bind both the receptors.

Fig. 4 Drug-induced acetylation of histone and nonhistone proteins in NB4 cells. (**A**) Cells were incubated for 6 hrs without/with 2 μM (S)-**2** or (R)-**2** or **4**, and then processed by Western blot and immunostained for acetylated H3/H4; H3/H4 were the loading controls. Cell extracts were also analysed by immunoblotting for (**B**) acetylated forms of nonhistone proteins α-tubulin and p53 after 6 and 24 hrs of treatment, respectively; α-tubulin and p53 were used as the reference proteins. (**C**) Drug-induced inhibition of human recombinant HDAC1 and HDAC6 activity was determined by a fluorimetric cell-free assay (Supporting Information, S2); IC_{50} values were from a typical experiment out of three.

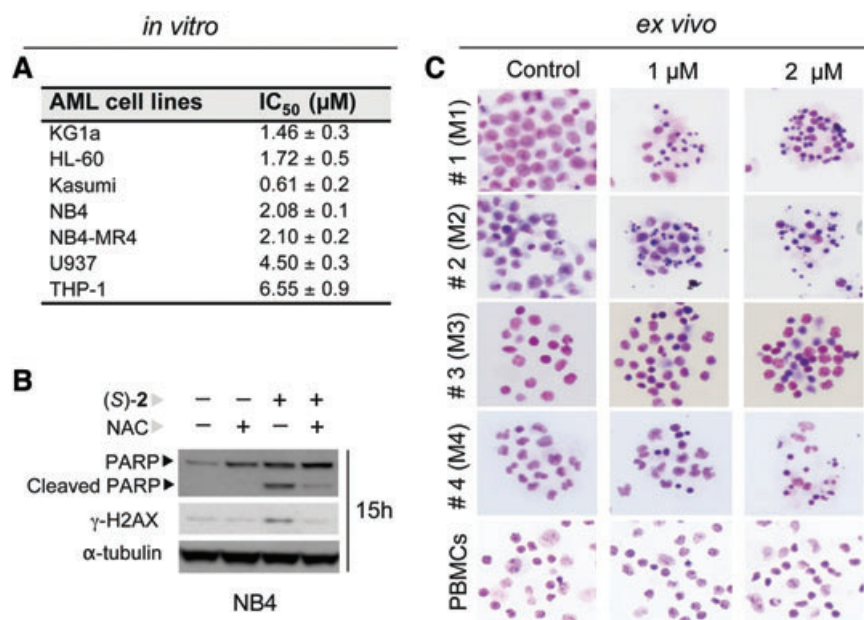| Compd	IC$_{50}$ (μM) *	
	HDAC1	HDAC6
(S)-2	0.75	2.70
(R)-2	2.18	7.08
4	2.15	3.35

* enzyme inhibition

Fig. 5 (S)-2 triggers apoptosis in different cultured and primary AML cells. (**A**) Different AML cell lines were treated for 2 days without/with increasing (S)-2 concentrations and then submitted to the Annexinn V/PI assay to determine the amount of apoptotic cells within the population. IC_{50} values represent the drug concentration (μM) needed for inducing 50% of cell population toward apoptosis relative to control; values were the means ± SD of three separate experiments. (**B**) Pro-apoptotic effects of (S)-2 in NB4 cells developed through the drug-mediated generation of ROS. Activation of apoptosis was revealed at 15 hrs, by the cleavage of PARP and phosphorylation of H2AX protein; and these events were efficiently contrasted by 15 mM N-Acetyl Cysteine (NAC) applied 2 hrs before drug addition; α-tubulin was used as the reference protein. (**C**) Ex vivo experiments on human different primary AML cells. May-Grünwald/Giemsa stained cytosmears of blasts (magnification: ×200) from peripheral blood of four newly diagnosed AML patients with M1, M2, M3 and M4 subtypes after 48 hrs of treatment without/with 1 and 2 μM drug. Peripheral blood mononuclear cells (PBMCs) from normal donors have also been isolated and treated as above after a 12-hr stimulation with PHA (125 μg/ml) and IL-2 (1 ng/ml).
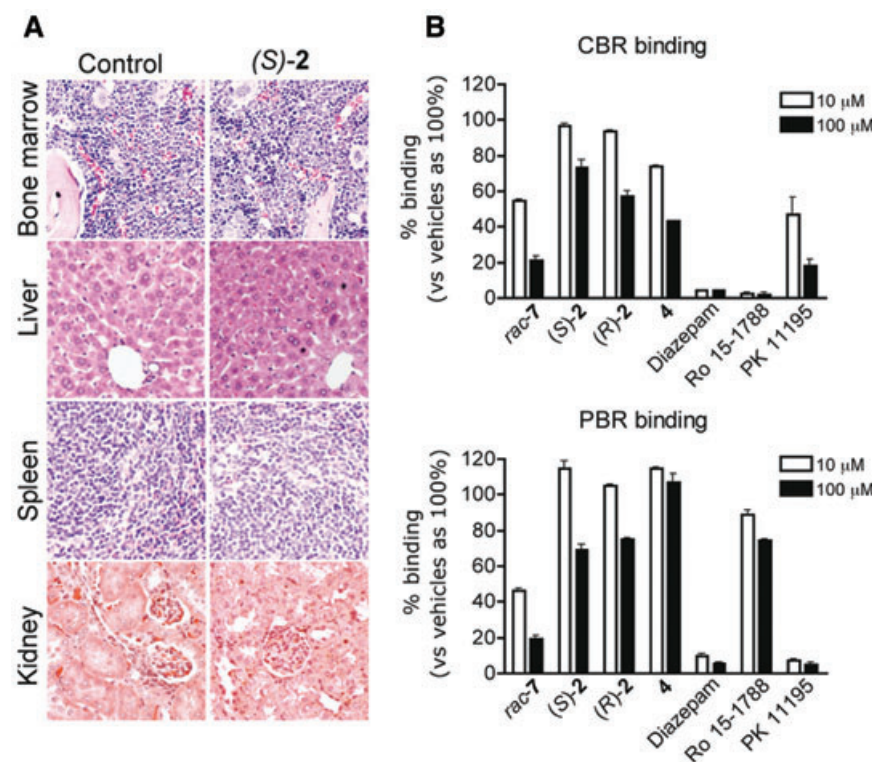

Fig. 6 (**A**) (S)-2 is well tolerated in normal CD-1 mice which have been used as the model for acute toxicity experiments. Animals were injected i.p. only once with increasing (S)-2 concentrations dissolved in 0.1 ml DMSO and sacrificed after a week (see Supporting Information, S3). Pictures (magnification: ×200) reported in this panel concern the histopathology of organs explanted from mice which were treated with the higher drug dosage, i.e. 150 mg/kg, corresponding to about 5 mg/mouse. No specific drug-induced tissue alteration in treated versus mice treated with the vehicle alone was observed. Consecutive 2.5–5 μm sections of samples were stained with May-Grünwald/Giemsa and examined under a bright field microscope (Nikon Eclipse, mod. 50i) equipped with a digital camera (DS-5M USB2) (Nikon Instruments, Florence, Italy). (**B**) Binding experiments in tissue extracts. The affinity of novel HDACi, at the two concentrations used (10 and 100 μM, respectively) for CBR was assayed by using membranes from rat cerebral cortex that were prepared as described by Mehta and Shank [17], while for PBR, rat kidney mitochondrial membrane preparations as described by Miccoli et al. were employed [18]. Bars were the means ± SE of three separate experiments; for details see Supporting Information, S4.

Discussion

The compounds reported in this study were chosen for their peculiar chemico-biological properties: the strikingly high enantioselectivity of *(S)*-**2** relative to *(R)*-**2**, the eutomer being *(S)*-**2** enantiomer, and the interesting comparison between activities of chiral *(S)*-**2** and **(**R**)*-**2** *versus* their non-chiral analogue **4**.

The presence of a methyl group in position 3 on the BDZ nucleus was not so important for biological HDACi activity as *(S)*-**2** and, to a lesser extent, **4** produced similar effects in NB4 cells and these were namely: (*i*) G0/G1 cell cycle arrest, (*ii*) acetylation of histone H3/H4 and nonhistone proteins, (*iii*) cleavage of PARP and increased levels of γ-H2AX in response to drug-induced DNA damage. Altogether, these events led to a massive apoptosis that, on average, developed in all the different cultured and primary AML cells reported herein, within 2–3 days at low micromolar drug dosages. On the other hand, the orientation of the chiral group on the BDZ ring seemed to be crucial for determining how the cap interacts with the external domain of HDACs within the intracellular milieu and, eventually, conferring enantioselectivity; the *(S)* configuration is preferred over the *(R)* one.

As regards nonhistone proteins, enhanced levels of acetylated α-tubulin and acetylated p53 were detected in Western blots of cells treated with *(S)*-**2** or **4** to suggest that HDAC6 and HDAC1, respectively, were targeted by the two active HDACi, while *(R)*-**2** produced just a minor signal. Partially consistent with this, all the three hybrids were capable, albeit with different potency, of inhibiting enzymatic activity of recombinant HDAC1 and HDAC6 thus addressing these isoforms as sensitive targets of novel HDACi but also emphasizing that results of fluorimetric cell-free assays do not always necessarily reflect biological activities of a given HDACi in cell-based assays.

The majority of biological assays reported herein pointed to *(S)*-**2** as the lead compound to be challenged in different cultured and primary AML cells. It is worth noting that promyelocytic NB4 and NB4-MR4 cells despite their different genetic asset and responsiveness to ATRA displayed similar IC_{50} values around 2 μM; while U937 and THP1 showed two- to three-fold higher values. With regard to *ex vivo* conditions, *(S)*-**2** triggered apoptosis in blasts from patients with M1, M2, M3 and M4 AML subtype [12] at 1–2 μM dose, while normal PBMCs were virtually unaffected by the treatment.

Importantly, the present study provides preliminary evidence that pro-apoptotic effects of *(S)*-**2** in NB4 cells develop through the drug-mediated generation of ROS that induces DNA damage,

as denoted by the cleavage of PARP and increase in γ-H2AX levels. Both these events were effectively prevented by the addition of the antioxidant N-acetyl-cysteine.

The results presented in this work concern the activities of novel HDACi used alone, well aware of the fact that their full anti-cancer potential in the clinic will derive from combination therapy with either standard anti-neoplastic agents or other experimental chemotherapies [9, 24]. Moreover, any HDACi to be employed *in vivo* should also be effective and safe. Regarding effectiveness, *(S)*-**2** displayed HDACi activities that were similar to those of SAHA [11] and, in terms of safety, results of acute toxicity experiments show that *(S)*-**2** was well tolerated in CD-1 mice up to very high dosage.

Overall, our findings have proven the powerful cytostatic and pro-apoptotic properties of the novel BDZ-hydroxamate *(S)*-**2** in different cultured and primary AML cells as well as its low-toxic profile *in vivo*, and pointed to this drug as a useful epigenetic tool to support standard therapy for the treatment of AML and, possibly, other types of haematological and solid malignancies.

Acknowledgements

Conflict of interest statement

The authors confirm that there are no conflicts of interest.

Supporting Information

Additional Supporting Information may be found in the online version of this article.

Please note: Wiley-Blackwell are not responsible for the content or functionality of any supporting materials supplied by the authors. Any queries (other than missing material) should be directed to the corresponding author for the article.

References

1. **Marks P, Rifkind RA, Richon VM,** *et al.* Histone deacetylases and cancer: causes and therapies. *Nat Rev Cancer*. 2001; 1: 194–202.

2. **Kouzarides T.** Histone acetylases and deacetylases in cell proliferation. *Curr Opin Genet Dev*. 1999; 9: 40–8.

3. **Monneret C.** Histone deacetylase inhibitors. *Eur J Med Chem*. 2005; 40: 1–13.

4. **Bolden JE, Peart MJ, Johnstone RW.** Anticancer activities of histone deacetylase inhibitors. *Nat Rev Drug Discov*. 2006; 5: 769–84.

5. **Marks PA, Xu WS.** Histone deacetylase inhibitors: potential in cancer therapy. *J Cell Biochem*. 2009; 107: 600–8.

6. **Mai A, Altucci L.** Epi-drugs to fight cancer: from chemistry to cancer treatment, the road ahead. *Int J Biochem Cell Biol*. 2009; 41: 199–213.

7. **Glozak MA, Sengupta N, Zhang X, *et al.*** Acetylation and deacetylation of non-histone proteins. *Gene*. 2005; 363: 15–23.

8. **Dokmanovic M, Marks PA.** Prospects: histone deacetylase inhibitors. *J Cell Biochem*. 2005; 96: 293–304.

9. **Bots M, Johnstone RW.** Rational combinations using HDAC inhibitors. *Clin Cancer Res*. 2009; 15: 3970–7.

10. **Marquard L, Poulsen CB, Gjerdrum LM, *et al.*** Histone deacetylase 1, 2, 6 and acetylated histone H4 in B- and T-cell lymphomas. *Histopathology*. 2009; 54: 688–98.

11. **Guandalini L, Cellai C, Laurenzana A, *et al.*** Design, synthesis and preliminary biological evaluation of new hydroxamate histone deacetylase inhibitors as potential antileukemic agents. *Bioorg Med Chem Lett*. 2008; 18: 5071–4.

12. **Bennett JM, Catovsky D, Daniel MT, *et al.*** Proposed revised criteria for the classification of acute myeloid leukemia. A report of the French-American-British Cooperative Group. *Ann Intern Med*. 1985; 103: 620–5.

13. **Laurenzana A, Cellai C, Vannucchi AM, *et al.*** WEB-2086 and WEB-2170 trigger apoptosis in both ATRA-sensitive and -resistant promyelocytic leukemia cells and greatly enhance ATRA differentiation potential. *Leukemia*. 2005; 19: 390–5.

14. **Cellai C, Laurenzana A, Bianchi E, *et al.*** Mechanistic insight into WEB-2170-induced apoptosis in human acute myelogenous leukemia cells: the crucial role of PTEN. *Exp Hematol*. 2009; 37: 1176–85.

15. **Paoletti F, Mocali A, Cellai C, *et al.*** Megakaryocyte-like increase in ploidy of Friend's erythroleukemia cells induced to endoreplication by colcemid. *Exp Hematol*. 1996; 24: 1441–8.

16. **Su H, Yu L, Nebbioso A, *et al.*** Novel N-hydroxybenzamide-based HDAC inhibitors with branched CAP group. *Bioorg Med Chem Lett*. 2009; 19: 6284–8.

17. **Mehta AK, Shank RP.** Characterization of a benzodiazepine receptor site with exceptionally high affinity for Ro 15–4513 in the rat CNS. *Brain Res*. 1995; 704: 289–97.

18. **Miccoli L, Oudard S, Beurdeley-Thomas A, *et al.*** Effect of 1-(2-chlorophenyl)-N-methyl-N-(1-methylpropyl)-3-isoquinoline carboxamide (PK11195), a specific ligand of the peripheral benzodiazepine receptor, on the lipid fluidity of mitochondria in human glioma cells. *Biochem Pharmacol*. 1999; 58: 715–21.

19. **Munson PJ, Rodbard D.** Ligand: a versatile computerized approach for characterization of ligand-binding systems. *Anal Biochem*. 1980; 107: 220–39.

20. **Sonoda H, Nishida K, Yoshioka T, *et al.*** Oxamflatin: a novel compound which reverses malignant phenotype to normal one *via* induction of JunD. *Oncogene*. 1996; 13: 143–9.

21. **Bonner WM, Redon CE, Dickey JS, *et al.*** GammaH2AX and cancer. *Nat Rev Cancer*. 2008; 8: 957–67.

22. **Lee YS, Lim KH, Guo X, *et al.*** The cytoplasmic deacetylase HDAC6 is required for efficient oncogenic tumorigenesis. *Cancer Res*. 2008; 68: 7561–9.

23. **Luo J, Su F, Chen D, *et al.*** Deacetylation of p53 modulates its effect on cell growth and apoptosis. *Nature*. 2000; 408: 377–81.

24. **Jones PA, Baylin SB.** The epigenomics of cancer. *Cell*. 2007; 128: 683–92.

25. **Cellai C, Laurenzana A, Vannucchi AM, *et al.*** Specific PAF antagonist WEB-2086 induces terminal differentiation of murine and human leukemia cells. *FASEB J*. 2002; 16: 733–5.

Author Query

Q1 Author: Figure 2 is in poor qulity. Please provide better quality figure.